

Electrical-optical analysis of photonic crystals GaN-based high power light emitting diodes

Meng Liu^{1,2} · Kang Li¹ · Fan-min Kong¹ · Jia Zhao¹ ·
Qing-an Ding³ · Ming-yu Zhang^{1,4}

Received: 22 October 2015 / Accepted: 22 March 2016 / Published online: 6 April 2016
© Springer Science+Business Media New York 2016

Abstract Although photonic crystals (PhCs) have been used to enhance the light extraction efficiency (LEE) of light emitting diodes (LEDs) in a lot of researches, the effects of PhCs on the electrical and optical characteristics of GaN-based high power LEDs have been rarely analyzed simultaneously. Herein, the 3D finite-element method (FEM) was employed to investigate the current density distribution in the active layer of LEDs while the LEE was calculated based on the finite-difference time-domain method. Then the influences of several parameters, including the radius, the filling factor, and the etching depth of PhCs on the current density distribution and external quantum efficiency (EQE) of LEDs were examined. It was found that the configurations of PhCs had a significant influence on the electrical and optical performances of LEDs. With the optimized parameters, a 62 % enhancement of EQE and more uniform current density distribution have been obtained comparing to those of LEDs with planar ITO. These analysis results can facilitate the identification of the design rules for high power, high efficiency LEDs.

Keywords External quantum efficiency (EQE) · Current density distribution · Photonic crystals (PhCs) · Light emitting diodes (LEDs)

✉ Kang Li
kangli@sdu.edu.cn

¹ School of Information Science and Engineering, Shandong University, Jinan 250100, China

² School of Physics and Electronics Engineering, Qilu Normal University, Jinan 250200, China

³ School of Information and Electrical Engineering, Shandong University of Science and Technology, Qingdao 266500, China

⁴ School of Information and Electrical Engineering, Shandong Jianzhu University, Jinan 250101, China

1 Introduction

In recent years, regarded as the next-generation lighting source, LEDs have drawn considerable attentions. And significant progresses have been made in GaN-based LEDs over the last decade (Nakamura and Krames 2013; Pimputkar et al. 2009). However, there are still some critical issues must to be addressed before their widely use in high power applications (Crawford 2009). For example, the light emission efficiency of LEDs decreases dramatically when the injected current density higher than 10 A/cm^2 . This has usually been called the efficiency droop (Cho et al. 2013), which is a bottleneck to reach high power LEDs. As far as the efficiency droop is concerned, the LEDs emission efficiency becomes sensitive to the lateral current density distribution in the active region. And it has been reported that uniform current density distribution can be beneficial to reduce the efficiency droop (Ryu and Shim 2011). On the other hand, the limited LEE due to total internal reflection and Fresnel reflection of the emitted light at the interface between the semiconductor material and air is another obstacle in getting high efficiency LEDs (Wiesmann et al. 2009; Hsu et al. 2012).

In order to solve the problems of normal LEDs mentioned above, many researchers have fabricated indium-tin oxide (ITO) on the top side of LEDs to improve the current spreading ability and encouraging results have already been demonstrated (Liou et al. 2014; Liu et al. 2011). And several methods, such as creating nano-scale patterns on the ITO or (and) p-GaN were introduced to enhance the LEE (Oh et al. 2013; Wang et al. 2010). In particular, PhCs structures have been proved as an effective approach to increase the LEE of LEDs (Matioli and Weisbuch 2010; Gao et al. 2011; David et al. 2006; Leem et al. 2007; Wang et al. 2009). However, the influences of PhCs on the current density distribution and EQE have been rarely discussed.

This work attempted to investigate the influences of PhCs on the current density distribution and EQE of LEDs. The influences of several parameters, including the radius, the filling factor, and the etching depth of PhCs have been explored. And a careful optimization of PhCs configurations has been presented. With the optimized structure, a 62 % enhancement of EQE and more uniform current density distribution have been realized. As the electrical and optical characteristics of high power PhCs LEDs were analyzed simultaneously in this paper, this will do a good favor for the design of high power, high efficiency LEDs.

2 Model of simulation and numerical methods

The schematic model of the simulated structure was depicted in Fig. 1. Balancing the accuracy of results and the computational cost, a calculation domain of $4 \mu\text{m} \times 4 \mu\text{m} \times 3.6 \mu\text{m}$ has been chosen since it has been demonstrated that a bigger model would have little effect on the LEE (Gao et al. 2011). The LEDs epitaxial layer structures were grown on a sapphire substrate. Above sapphire substrate was the $1.8 \mu\text{m}$ n-GaN layer. Then the active layer (MQWs) and a 200 nm-thick p-GaN layer were subsequently grown. Above p-GaN layer was the ITO current spreading layer. A mesa structure has been etched to expose the n-GaN layer in order to deposit the n-contact. The p- and n-contacts with diameter 1 and $2 \mu\text{m}$ were formed from the corner of the LEDs chip, respectively. And the parameters used in simulations were shown in Table 1.

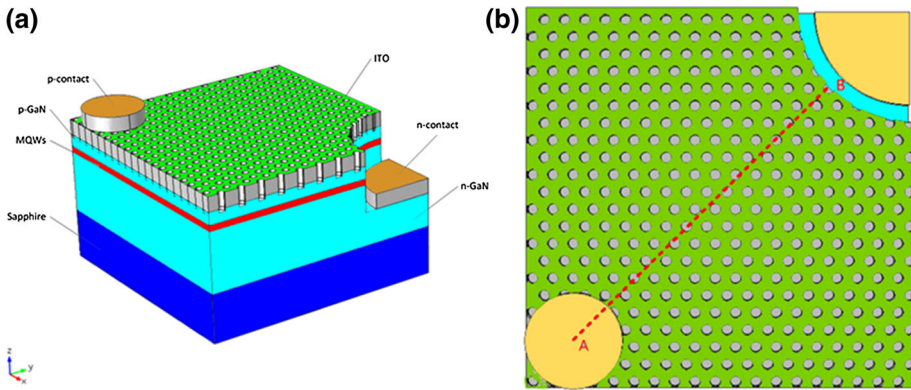


Fig. 1 **a** The schematic model of PhCs LEDs used in simulation and **b** the top view of the model, the red dash line represented a reference line in the active layer

Table 1 Parameters of epi-layers used in simulations

Epi-layer	Height (μm)	Electrical conductivity (s/m)	Refractive index
p-contact/n-contact	0.25	1e15	–
ITO	0.25	1e7	2.0
p-GaN	0.2	35	2.5
MQWs	0.1	1e3	2.5
n-GaN	1.8	1e4	2.5
Sapphire	1.0	–	1.7

In order to investigate the effect of PhCs structure on the current density distribution in LEDs, we developed a 3D electrical model using FEM numerical simulation. As we know, the current–voltage characteristic of the p–n junction can be described by the Shockley equation:

$$J_e = J_s \left[\exp\left(\frac{eV_j}{nkT}\right) - 1 \right] \tag{1}$$

where J_s is the saturation current density, n is the ideality factor, V_j is the voltage drop of the p–n junction and T is the absolute temperature, which is assumed to be 300 K. And the current density of the p–n junction follows the continuity equation for electronic transport:

$$\nabla \cdot \overline{J(r)} + \frac{\partial n}{\partial t} = 0 \tag{2}$$

where $\overline{J(r)}$ is the current density as a function of position r and $\partial n/\partial t$ is the change rate in the carrier concentration.

During the simulations, a current of 0.02 mA was injected into LEDs through the p-contact, and the n-contact was set as ground. So the current density in the epitaxial layers was about 125 A/cm². As it has been proved in Huang et al. (2010), while high current

injected into LEDs, the resistance characteristic of the p–n junction dominated, therefore, we used an equivalent resistance to simulate the current behavior in the active layer:

$$V_j = \rho_a d_a J(r) + V_0 \tag{3}$$

where ρ_a is the electrical resistivity of the p–n junction, d_a is the thickness of the p–n junction and V_0 is a positive fitting constant. Then, for the sake of simplicity, the details of the MQW and barriers were ignored, and the MQWs were equivalent as resistance with 100 nm thickness.

As far as the other epi-layers were concerned, we neglected the carriers’ recombination processes, their electronic characteristics followed the Ohm’s law:

$$\overline{J}(r) = -\sigma \cdot \nabla \varphi \tag{4}$$

where φ and σ denote the electric potential and the electrical conductivity of the material, respectively.

Insulated boundary conditions except for the p- and n-contacts have been chosen during the simulations. Metal contact boundary conditions were applied to the p- and n-contacts in order to apply voltage and current biases to the device. And all interfaces between the contacts, ITO and semiconductor layers were assumed to be Ohmic contacts.

While the simulation model has been built, just as most researches have done (Hwang and Shim 2008; Bogdanov et al. 2010), a reference line as shown by a red dash line A–B in Fig. 1b across the chip has been chosen to represent the active layer characteristics in the best possible way. Then the current density uniformity can be characterized by the standard deviation of the current density along the reference line (Xue et al. 2014):

$$\sigma_j = \sqrt{\frac{1}{n-1} \sum_{i=1}^n (J_i - \bar{J})^2} \tag{5}$$

where $\bar{J} = \frac{1}{n} \sum_{i=1}^n J_i$ is the average current density.

As has been proofed by Ryu et al. (2009), the IQE at arbitrary current density J can be expressed as

$$\eta_{IQE} = 1 - \frac{(1 - \eta_{max})}{2J} \left(1 + \frac{\eta_{IQE} J}{\eta_{max} J_{max}} \right) \sqrt{\frac{\eta_{IQE} J J_{max}}{\eta_{max}}} \tag{6}$$

where η_{max} is the maximum value of IQE at the corresponding current density J_{max} .

We also used the FDTD method to calculate the LEE of PhCs LEDs. As we know, dipole sources were best suited for excitation since it has been proved that the electron–hole recombination can be classically represented by a dipole source (Wiesmann 2009; Benisty et al. 1998). However, it was worth noting that since the FDTD was intrinsically a coherent simulation method, using multiple dipole sources in one simulation domain as well as periodic continuation boundary conditions was not convenient, because it would lead to an unphysical interference pattern. Therefore, a single dipole source within the computational domain was chosen which was also adopted by many other numerical studies (Ding et al. 2014; Wang et al. 2012). Furthermore, it has been proved that the results corresponding to the position of the dipole source within the active layer have only negligible difference on the LEE (Gao et al. 2011). Hence, to simplify the whole simulation, we used an in–plain polarized point dipole with a wavelength of 465 nm located

450 nm below the ITO–air interface as a radiating source of LEDs. In order to get a precise result, we have located the dipole in two different places, such as under and not under the PhCs, and then the average result of these two different places was used to represent that of the active layer in simulations. In addition, inhomogeneous mesh was used during the simulations, and the initial minimum grid was set to 5 nm while the maximum was 20 nm. Furthermore, a perfectly matched layer (PML) (Sacks et al. 1995) enclosing the entire simulation domain was used as the absorbing boundary during the simulations. The PML could absorb any radiation that reached the boundaries of the simulation domain, and effectively eliminate any reflection at the boundaries that could interfere with the simulation. A schematic of the FDTD computational domain was shown in Fig. 2.

The LEE was estimated as the ratio of the power flux extracted from the top side of LEDs (P_{out}) with respect to the overall emitted power from the source (P_{source}) (Wiesmann 2009):

$$\eta_{LEE} = \frac{P_{out}}{P_{source}} \quad (7)$$

The EQE can be expressed as

$$\eta_{EQE} = \eta_{LEE} \cdot \eta_{IQE} \quad (8)$$

And the EQE enhancement factor F was defined as

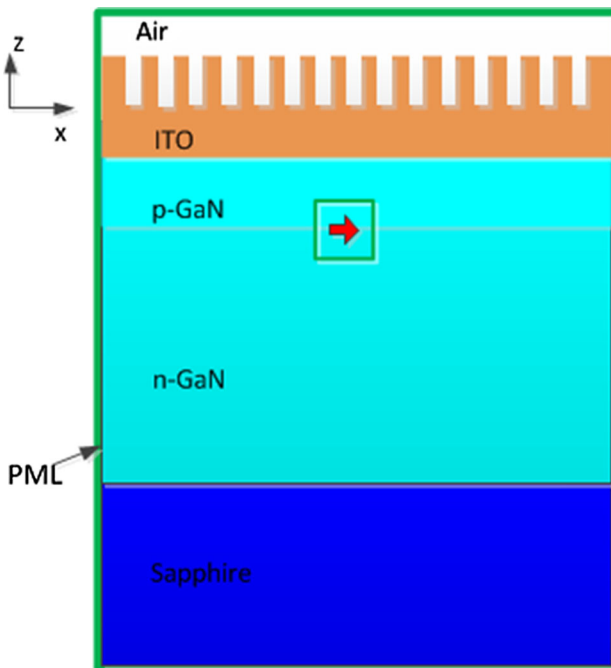


Fig. 2 Schematic of the computational domain of LEDs

$$F = \frac{\eta_{EQE} - \eta_0}{\eta_0} \times 100 \% \quad (9)$$

where η_{EQE} was the EQE of PhCs LEDs and η_0 was the EQE of planar ITO LEDs.

3 Results and discussion

3.1 Current density distribution in the active layer of LEDs

In the first place, the current density along the typical reference A-B dash line in the active layer of normal planar LEDs was calculated and normalized to the corresponding maximum value, and the results were shown in Fig. 3a. From Fig. 3a, we can find a huge current crowding near the p-contact. That was because that the current could not spread freely into the whole active layer region due to the large resistance of p-GaN, conversely, concentrated in the region under the p-contact and the current spreading length was very short.

While the ITO current spreading layer was fabricated on the p-GaN layer, the current could travel further across the ITO layer because of the high conductivity of the ITO layer. However, the current density distribution was still non-uniform and the current crowded near the n-contact instead (see Fig. 3b). It seemed that the current would crowd near either p- or n-contact and hardly to be uniform. This phenomenon occurred because current tended to pass through LEDs via the path with the smallest resistance between the n- and p-contact (Guo and Schubert 2001). However, the series resistance of the lateral current paths was difficult to match perfectly. When PhCs were fabricated on the top layer of LEDs, the conductivity of ITO layer was a little reduced, and as the PhCs structure was optimized, the more matching series resistance for the lateral current path maybe realized, that was $R_{ITO} \approx R_{n-GaN}$, and consequently a more uniform current density distribution could be achieved. This conclusion agreed well with the theoretical predictions of Chen et al. (2009).

The normalized current density of LEDs with normal PhCs and optimized PhCs were also shown in Fig. 3b for comparison. Here, the radius and depth of the normal PhCs were set as 60 nm and 300 nm, respectively, while the filling factor was 0.2. And those of the optimized PhCs were set as 60 nm, 300 nm and 0.4, respectively. From Fig. 3b, we could

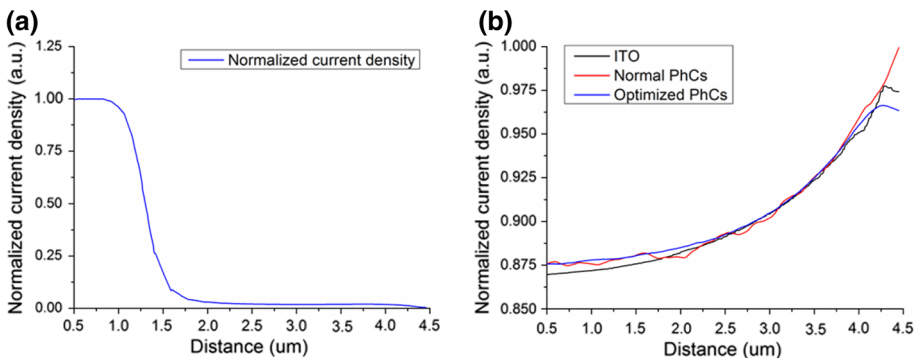


Fig. 3 The current density distribution in the active layer of **a** normal planar LEDs and **b** planar ITO LEDs, normal PhCs LEDs and optimized PhCs LEDs

find that the current density distribution of these three LEDs were similar with that of Li et al. (2014) and the difference between them was not obvious, however, LEDs with normal PhCs had a high current density fluctuation, and the standard deviation of the normalized current density was 0.038. So the current density distribution was a little degraded comparing with that of the planar ITO LEDs 0.032. However, as the PhCs structure was optimized, the current density near the p-contact increased while that near the n-contact decreased, so a little more uniform than the planar ITO LEDs has been obtained. And the standard deviation of the normalized current density was 0.025 as has been calculated.

3.2 The influence of dipole position on the LEE while the current crowding effect and p/n-contacts absorption are considered

Before studying the influences of PhCs configurations on the EQE, we firstly studied the influence of dipole position on the LEE when current crowding effect and p-/n-contacts absorption were considered. Here, a 3D normal planar LEDs model was established as an example. We selected forty points equally spaced along the reference line shown in Fig. 1b and got the current density of these points. Then the active layer was represented by dipoles placed at these points. One dipole was chosen once in a simulation to avoid the unphysical interference pattern. The influence of dipole position on the LEE was shown in Fig. 4a.

The simulation results illustrated that rays emitted from the dipole under the p-contact had very low LEE because of the absorption of p-contact, while those not under the contact had almost uniform LEE. That meant current crowding near n-contact had little influence on the LEE, while current crowding near p-contact resulted in a notable LEE droop due to the significant absorption of rays emitted under p-contact. And this was in good agreement with the conclusion of Cao et al. (2013). So in the following simulations, as the ITO current spreading layer has been added, n-contact current crowding occurred. Accordingly, we used a dipole located in the center of the active layer to represent the source for simplicity, and the absorption of p-contact was neglected.

In addition, the power loss due to material absorption during the simulation was also ignored since the extinction coefficient of GaN and ITO are closed to zero at the wavelength of 465 nm as shown in Fig. 4b (Köhler 1999; Synowicki 1998).

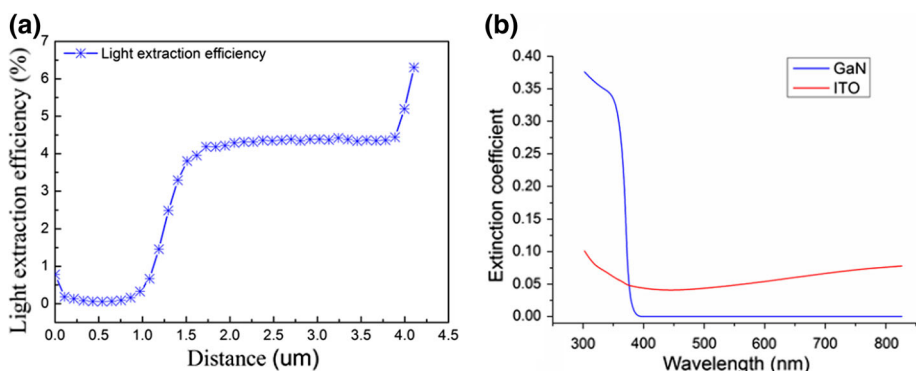


Fig. 4 **a** The influence of dipole position on the LEE and **b** the extinction coefficient of GaN and ITO

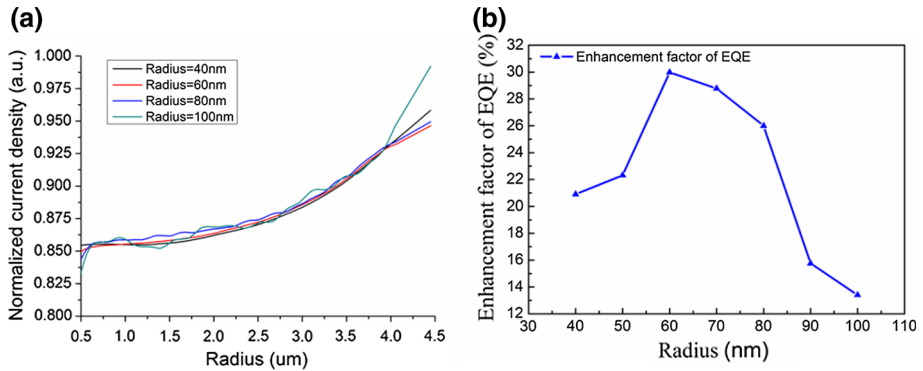


Fig. 5 Influences of PhCs radius on the current density distribution and EQE

3.3 Influences of PhCs radius on the current density distribution and EQE of LEDs

Then the influences of PhCs parameters such as the radius, the filling factor, and the depth on the current density distribution and EQE of LEDs were investigated. During the simulations, PhCs parameters were varied in turn while the other parameters were kept constant, and the current density distribution and enhancement of EQE was calculated.

Firstly, we considered the effect of PhCs radius on the current density distribution and EQE. For this purpose, hexagonal PhCs with radius varied from 40 nm to 100 nm in steps of 10 nm were simulated and compared. In general, the filling factor and the PhCs depth were temporarily selected to be 0.33 and 300 nm, respectively. And the results were shown in Fig. 5. To be clear, there were only four lines shown in Fig. 5.

As have been calculated, the standard deviations of the normalized current density of LEDs with PhCs radius varied from 40 nm to 100 nm were about 0.031, 0.032, 0.041, and 0.058, respectively. These results showed that the current density uniformity of LEDs became better with the decrease of PhCs radius and those with 40 nm radius offered the best current uniformity.

Based on the current density in the active layer from electrical simulation, the IQE for each case was then calculated using formula (6), considering the maximum η_{IQE} of about 80 % when the current density was 10 A/cm² for GaN-based LEDs (Cao et al. 2013). And

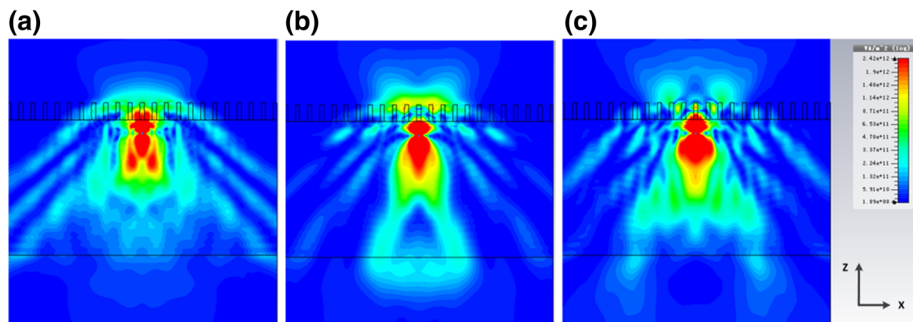


Fig. 6 The cross-section view of power flow of LEDs with **a** radius = 40 nm, **b** radius = 60 nm, **c** radius = 80 nm

the LEE was computed by FDTD method too. Then the EQE was obtained from formula (8). From the results shown in Fig. 5b, we could find that the best EQE was obtained when the PhCs radius equaled 60 nm. This could be manifested by the power flow intensity of LEDs.

Figure 6 showed the cross-section view of power flow of LEDs with radius equaled 40 nm, 60 nm and 80 nm, respectively. From Fig. 6, we could find that the largest intensity of power flow was obtained when PhCs radius equaled 60 nm, as the guide modes were most effectively diffracted. When radius = 40 nm, there was a broad power flow, however, the intensity of the power was very weak. And while radius = 80 nm, very little light power have been diffracted out of the LEDs.

3.4 Influences of PhCs filling factor on the current density distribution and EQE of LEDs

Then the influences of PhCs filling factor on the current density distribution and EQE of LEDs were calculated while keeping the PhCs depth equaled 300 nm and the PhCs radius equaled 60 nm, at which the maximum EQE was obtained from the above simulation. And the results were shown in Fig. 7. From the calculated results, the standard deviations of the normalized current density of LEDs with PhCs filling factor varied from 0.2 to 0.5 with a 0.1 increment were about 0.038, 0.033, 0.032, and 0.029, respectively. This meant that the current density uniformity rose with the increase of PhCs filling factor. This could be explained by the effective medium theory. And the effective conductivity σ_{eff} could be obtained by (Yu and Wu 2010)

$$\sigma_{eff} = \chi_1\sigma_1 + \chi_2\sigma_2 \tag{10}$$

where $\chi_1 + \chi_2 = 1$, χ_1 and χ_2 were the volume fractions of ITO and air, respectively, while σ_1 and σ_2 were conductivities of these two materials.

In order to explain the simulation results, the equivalent circuit model of the top layer for LEDs was constructed. As shown in Fig. 8, $R_{PhCs-ITO}$, R_{ITO} were the resistance of the ITO with and without of PhCs, and $R_{PhCs-p-GaN}$, R_{p-GaN} were the resistance of the p-GaN with and without of PhCs, respectively. I_1 , I_2 , and I_3 represented the current flowing through a certain region. Then the effective resistance could be represented by the shunt of the certain layers resistances. As the depth of PhCs has been fixed at 300 nm, where ITO has been just etched through, the volume fractions were depended on the filling factor of

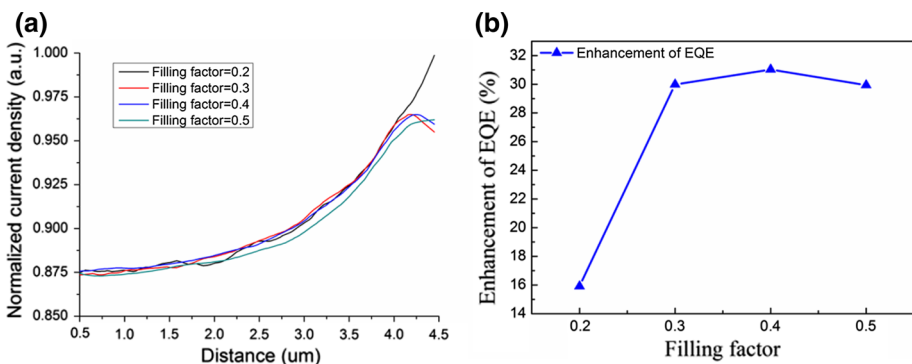


Fig. 7 Influences of PhCs filling factor on the current density distribution and EQE

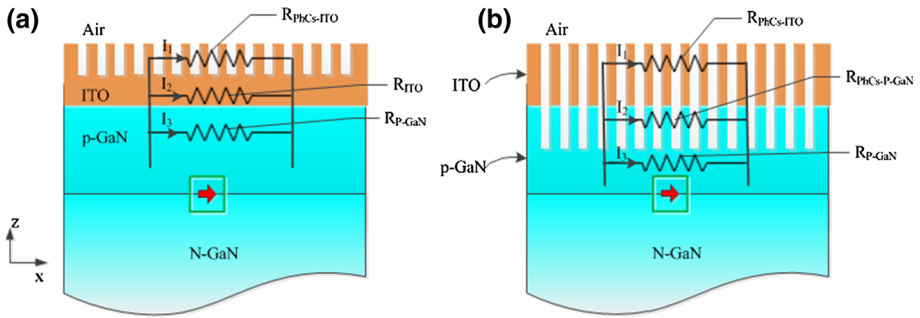


Fig. 8 The equivalent circuit model of the top layer for **a** ITO shallow etched LEDs, **b** LEDs with ITO etched through

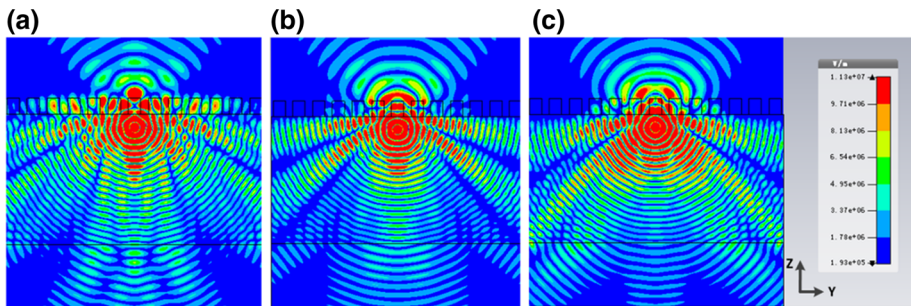


Fig. 9 The electric field intensity distribution of LEDs with filling factor **a** 0.3, **b** 0.4 and **c** 0.5

PhCs. When the filling factor of PhCs increased, the $R_{PhCs-ITO}$, R_{p-GaN} , and $R_{PhCs-p-GaN}$ increased too. And the conductivity of the top layer would decrease correspondingly, so the difference of series resistance between the top layer and the n-GaN layer decreased. This would do a good favor for the uniformity of current density distribution.

However as far as the EQE was concerned, LEDs with filling factor equaled 0.4 showed the best performance. Figure 9 gave the electric field intensity distribution of LEDs with filling factor varied from 0.3 to 0.5. From Fig. 9, we could find that although the PhCs with filling factor equals 0.3 have more interaction with the guided modes, however, the guided modes have not been diffracted out effectively. And according to the effective dielectric theory (Yeh et al. 1976), the effective refractive index of PhCs layer could be expressed as (Matioli 2010):

$$n_{PhCs} = \sqrt{fn_{air}^2 + (1-f)n_{ITO}^2} \tag{11}$$

where f was the filling factor of PhCs. And the calculated effective refractive indexes of the PhCs layer in ITO of these three kinds of LEDs were 1.76, 1.67 and 1.58, respectively, while that of the PhCs layer in p-GaN were 2.16, 2.03 and 1.9, respectively. Obviously, when the filling factor equaled 0.4, the more optimal refractive index matching has been achieved, which could be regarded as a grade-refractive-index antireflection coating, that was:

$$n_{p-GaNPhCs}^2 \approx n_{GaN} \times n_{ITOPhCs} \tag{12}$$

Then the highest transmittance would be obtained, therefore when the filling factor equals 0.4, the best performance has been achieved.

3.5 Influences of PhCs depth on the current density distribution and EQE of LEDs

Then the filling factor and radius of PhCs were fixed at 0.4 and 60 nm respectively, we calculated the influence of PhCs depth on the current density distribution and EQE of LEDs with PhCs depth varied from 50 nm to 400 nm in steps of 50 nm, and the results were shown in Fig. 10. To be clear, only four lines have been given in Fig. 10a. From the results that have been calculated, the standard deviations of the normalized current density of LEDs shown above were about 0.034, 0.025, 0.031, and 0.047, respectively. These results implied that the current density uniformity firstly rose with the increase of PhCs etching depth, and got the best uniformity when the PhCs have just etched through the ITO with the p-GaN a little shallow etched too, that was, depth ~ 300 nm. Then as p-GaN layer etched further, the uniformity of the current density became worse and worse. This also can be explained by the effective conductivity.

As demonstrated in Fig. 8a, when the ITO was shallow etched, the effective resistance was depended on the resistance of the ITO layer and I_2 was the main current. As the depth of PhCs increased, the conductivity of the ITO layer decreased and became closer to the conductivity of the n-GaN layer, the uniformity of current density distribution got better. However, when the ITO layer has been etched through, the influence of the p-GaN layer became more and more critical and I_1 became the main current. The effective conductivity decreased drastically as the degradation of the p-GaN etching (Pearson et al. 1999), and then the uniformity of the current density became worse. From Fig. 10a, we can find that when the PhCs depth equalled 400 nm, as the p-GaN layer nearly also etched through, the electrical conductivity was degraded gravely, and therefore, the current density distribution fluctuated more severely.

From Fig. 10b, we could find that while the EQE was concerned, LEDs with etching depth ~ 350 nm lead to a considerable enhancement of light emission. However, as we know, with the etching depth increasing, PhCs should have more interaction with the guide modes, and the light emission may stronger. In order to explain this phenomenon, the transmittance of LEDs with different depth PhCs has been calculated through rigorous coupled-wave analysis, and the results were shown in Fig. 11. As shown in Fig. 11, the transmittance of LEDs with PhCs 350 nm etched was much larger than that of LEDs with

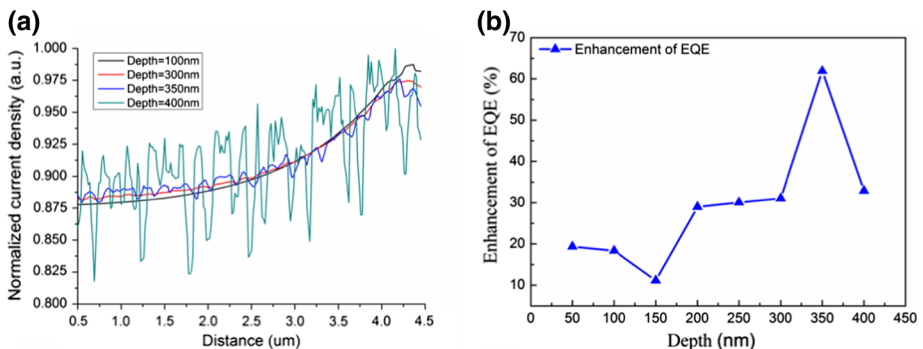


Fig. 10 Influences of PhCs depth on the current density distribution and EQE

Fig. 11 The transmittance of LEDs with different depth PhCs

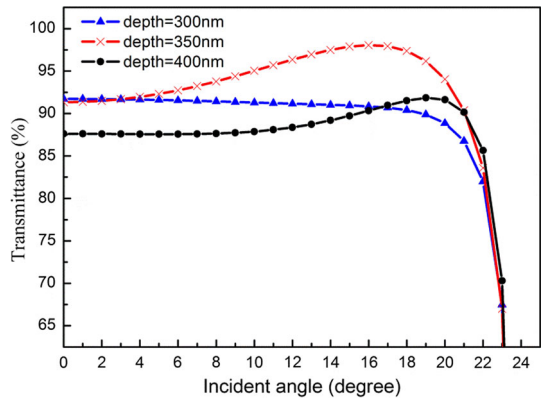
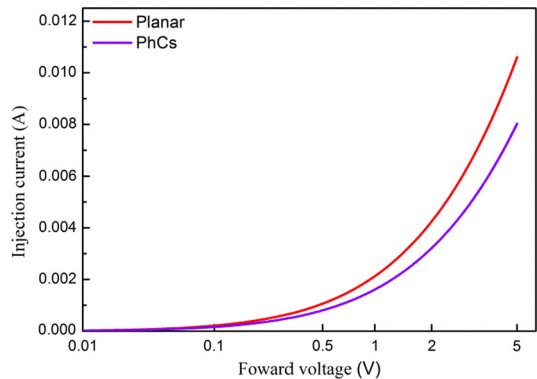


Fig. 12 The comparison of current–voltage (I – V) characteristics of planar and PhCs LEDs



300 nm and 400 nm depth PhCs, this resulted in a good enhancement of light emission. And the results indicated that the EQE of LEDs with optimized PhCs achieved an enhancement of 62 % compared to that of LEDs with planar ITO.

In addition, as the PhCs have been etched on the top of the LEDs, it was inevitably increase the series resistance of the LEDs chip. Then, the forward voltage at a certain injection current would be larger than the planar LEDs. Nevertheless, considerable improvement in light output was still obtained from the above investigation. The comparison of the forward voltage of the planar and PhCs LEDs were shown in Fig. 12. However, it was worth mention that, from Fig. 12, due to the simplification of the active layer during the simulation, we could also find a serious leakage current in both LEDs unfortunately, which should be improved in later research. Furthermore, the leakage current of PhCs LEDs was a little smaller than that of planar LEDs because of the more uniform current density distribution, and this was agree well with the conclusion in Morkoç et al. (2009).

4 Conclusion

The electrical and optical characteristics of high power PhCs LEDs have been simultaneously investigated in this paper. The significant influences of PhCs on the current density distribution and EQE of LEDs were demonstrated through simulations. Different PhCs

configurations were investigated in order to optimize the LEDs performances under high injection conditions. Data from the present study clearly indicated that when the PhCs structure was etched on the top layer of LEDs, the current density distribution was decreased in some cases. However, with the optimized parameters, a 62 % enhancement of EQE and more uniform current density distribution have been obtained comparing to those of LEDs with planar ITO because of the more matching series resistance for the lateral current path, more effective diffraction and more optimal refractive index matching. These analysis results will be beneficial to understand the effects of PhCs on electrical and optical characteristics of LEDs and therefore lead to high power, high efficiency LEDs for practical applications in future solid-state lighting.

Acknowledgments This work is supported by the National Natural Science Foundation of China (61077043, 61475084, 61327808) and the Fundamental Research Funds of Shandong University (2014JC032).

References

- Benisty, H., Stanley, R., Mayer, M.: Method of source terms for dipole emission modification in modes of arbitrary planar structures. *J. Opt. Soc. Am. A* **15**, 1192–1201 (1998)
- Bogdanov, M.V., Bulashevich, K.A., Khokhlev, O.V., Evstratov, I.Y., Ramm, M.S., Karpov, S.Y.: Current crowding effect on light extraction efficiency of thin-film LEDs. *Phys. Status Solidi (c)* **7**(7–8), 2124–2126 (2010). doi:[10.1002/pssc.200983415](https://doi.org/10.1002/pssc.200983415)
- Cao, B., Li, S., Hu, R., Zhou, S., Sun, Y., Gan, Z., Liu, S.: Effects of current crowding on light extraction efficiency of conventional GaN-based light-emitting diodes. *Opt. Express* **21**(21), 25381–25388 (2013). doi:[10.1364/oe.21.025381](https://doi.org/10.1364/oe.21.025381)
- Chen, J.-C., Sheu, G.-J., Hwu, F.-S., Chen, H.-I., Sheu, J.-K., Lee, T.-X., Sun, C.-C.: Electrical-optical analysis of a GaN_sapphire LED chip by considering the resistivity of the current-spreading layer. *Opt. Rev.* **16**(2), 213–215 (2009)
- Cho, J., Schubert, E.F., Kim, J.K.: Efficiency droop in light-emitting diodes: challenges and countermeasures. *Laser Photon. Rev.* **7**(3), 408–421 (2013). doi:[10.1002/lpor.201200025](https://doi.org/10.1002/lpor.201200025)
- Crawford, M.H.: LEDs for solid-state lighting-performance challenges and recent advances. *IEEE J. Sel. Top. Quantum Electron.* **15**(4), 1028–1040 (2009)
- David, A., Fujii, T., Sharma, R., McGroddy, K., Nakamura, S., DenBaars, S.P., Hu, E.L., Weisbuch, C., Benisty, H.: Photonic-crystal GaN light-emitting diodes with tailored guided modes distribution. *Appl. Phys. Lett.* **88**(6), 061124-1–061124-3 (2006). doi:[10.1063/1.2171475](https://doi.org/10.1063/1.2171475)
- Ding, Q.A., Li, K., Kong, F., Chen, X., Zhao, J.: Improving the vertical light-extraction efficiency of GaN-based thin-film flip-chip LEDs with p-side deep-hole photonic crystals. *J. Disp. Technol.* **10**(11), 909–916 (2014)
- Gao, H., Li, K., Kong, F.-M., Chen, X.-L., Zhang, Z.-M.: Improving light extraction efficiency of GaN-based LEDs by AlxGa1-xN confining layer and embedded photonic crystals. *IEEE J. Sel. Top. Quantum Electron.* **18**, 1650–1660 (2011)
- Guo, X., Schubert, E.F.: Current crowding and optical saturation effects in GaInN/GaN light-emitting diodes grown on insulating substrates. *Appl. Phys. Lett.* **78**(21), 3337 (2001). doi:[10.1063/1.1372359](https://doi.org/10.1063/1.1372359)
- Hsu, C.-W., Lee, Y.-C., Chen, H.-L., Chou, Y.-F.: Optimizing textured structures possessing both optical gradient and diffraction properties to increase the extraction efficiency of light-emitting diodes. *Photon. Nanostruct. Fundam. Appl.* **10**(4), 523–533 (2012). doi:[10.1016/j.photonics.2012.04.005](https://doi.org/10.1016/j.photonics.2012.04.005)
- Huang, S., Wu, H., Fan, B., Zhang, B., Wang, G.: A chip-level electrothermal-coupled design model for high-power light-emitting diodes. *J. Appl. Phys.* **107**(5), 054509-1–054509-8 (2010). doi:[10.1063/1.3311564](https://doi.org/10.1063/1.3311564)
- Hwang, S., Shim, J.: A method for current spreading analysis and electrode pattern design in light-emitting diodes. *IEEE Trans. Electron. Dev.* **55**(5), 1123–1128 (2008)
- Köhler, U., As, D.J., Schöttker, B., Frey, T., Lischka, K., Scheiner, J., Shokhovets, S., Goldhahn, R.: Optical constants of cubic GaN in the energy range of 1.5–3.7 eV. *J. Appl. Phys.* **85**(1), 404–407 (1999)

- Leem, D.-S., Lee, T., Seong, T.-Y.: Enhancement of the light output of GaN-based light-emitting diodes with surface-patterned ITO electrodes by maskless wet-etching. *Solid State Electron.* **51**(5), 793–796 (2007). doi:[10.1016/j.sse.2007.02.038](https://doi.org/10.1016/j.sse.2007.02.038)
- Li, C.-K., Rosmeulen, M., Simoen, E., Wu, Y.-R.: Study on the optimization for current spreading effect of lateral GaN/InGaN LEDs. *IEEE Trans. Electron Devices* **61**(2), 511–517 (2014)
- Liou, J.-K., Chen, C.-C., Chou, P.-C., Tsai, T.-Y., Cheng, S.-Y., Liu, W.-C.: Improved current spreading performance of a GaN-based light-emitting diode with a stair-like ITO layer. *Solid State Electron.* **99**, 21–24 (2014). doi:[10.1016/j.sse.2014.05.002](https://doi.org/10.1016/j.sse.2014.05.002)
- Liu, Y.J., Huang, C.C., Chen, T.Y., Hsu, C.S., Liou, J.K., Tsai, T.Y., Liu, W.C.: Implementation of an indium-tin-oxide (ITO) direct-Ohmic contact structure on a GaN-based light emitting diode. *Opt. Express* **19**(15), 14662–14670 (2011)
- Matioli, E.: Embedded photonic crystals for high-efficiency gan-based optoelectronic devices. PhD thesis, Materials Department, University of California, Santa Barbara (2010)
- Matioli, E., Weisbuch, C.: Impact of photonic crystals on LED light extraction efficiency: approaches and limits to vertical structure designs. *J. Phys. D Appl. Phys.* **43**(35), 354005-1–354005-22 (2010). doi:[10.1088/0022-3727/43/35/354005](https://doi.org/10.1088/0022-3727/43/35/354005)
- Morkoç, H., Shim, J.-I., Yun, J., Kim, H., Litton, C.W., Chyi, J.-I., Nanishi, Y., Piprek, J., Yoon, E.: Current spreading and its related issues in GaN-based light emitting diodes. *SPIE OPTO: integrated optoelectronic devices. Int. Soc. Opt. Photon.* **7216**, 72160V-72161–72160V-72169 (2009). doi:[10.1117/12.808393](https://doi.org/10.1117/12.808393)
- Nakamura, S., Krames, M.R.: History of gallium–nitride-based light-emitting diodes for illumination. *Proc. IEEE* **101**(10), 2211–2220 (2013)
- Oh, S., Su, P.-C., Yoon, Y.-J., Cho, S., Oh, J.-H., Seong, T.-Y., Kim, K.-K.: Nano-patterned dual-layer ITO electrode of high brightness blue light emitting diodes using maskless wet etching. *Opt. Express* **21**(S6), A970 (2013). doi:[10.1364/oe.21.00a970](https://doi.org/10.1364/oe.21.00a970)
- Pearnton, S.J., Zolper, J.C., Shul, R.J., Ren, F.: GaN: processing, defects, and devices. *J. Appl. Phys.* **86**(1), 1–78 (1999). doi:[10.1063/1.371145](https://doi.org/10.1063/1.371145)
- Pimputkar, S., Speck, J.S., DenBaars, S.P., Nakamura, S.: Prospects for LED lighting. *Nat. Photon.* **3**(4), 180–182 (2009)
- Ryu, H.-Y., Shim, J.-I.: Effect of current spreading on the efficiency droop of InGaN light-emitting diodes. *Opt. Express* **19**(4), 2886–2894 (2011)
- Ryu, H.-Y., Kim, H.-S., Shim, J.-I.: Rate equation analysis of efficiency droop in InGaN light-emitting diodes. *Appl. Phys. Lett.* **95**(8), 081114-1–081114-3 (2009). doi:[10.1063/1.3216578](https://doi.org/10.1063/1.3216578)
- Sacks, Z.S., Kingsland, D.M., Lee, R., Lee, J.: A perfectly matched anisotropic absorber for use as an absorbing boundary condition. *IEEE Trans. Antenn. Propag.* **43**, 1460–1463 (1995)
- Synowicki, R.A.: Spectroscopic ellipsometry characterization of indium tin oxide film microstructure and optical constants. *Thin Solid Films* **313**, 394–397 (1998)
- Wang, P., Gan, Z., Liu, S.: Improved light extraction of GaN-based light-emitting diodes with surface-patterned ITO. *Opt. Laser Technol.* **41**(6), 823–826 (2009). doi:[10.1016/j.optlastec.2008.12.008](https://doi.org/10.1016/j.optlastec.2008.12.008)
- Wang, P., Cao, B., Wei, W., Gan, Z., Liu, S.: Improved light extraction of GaN-based light-emitting diodes by ITO patterning with optimization design. *Solid State Electron.* **54**(3), 283–287 (2010). doi:[10.1016/j.sse.2009.10.005](https://doi.org/10.1016/j.sse.2009.10.005)
- Wang, X., Li, K., Kong, F., Zhang, Z.: Surface spherical crown arrays structure increases GaN-based LED efficiency. *Opt. Quantum Electron.* **45**(7), 611–616 (2012). doi:[10.1007/s11082-012-9644-2](https://doi.org/10.1007/s11082-012-9644-2)
- Wiesmann, C.: Nano-structured LEDs—light extraction mechanisms and applications. Ph.D. thesis, Science Faculty, Universität Regensburg, Regensburg, Germany, pp. 41–45 (2009)
- Wiesmann, C., Bergenek, K., Linder, N., Schwarz, U.T.: Photonic crystal LEDs—designing light extraction. *Laser Photon. Rev.* **3**(3), 262–286 (2009). doi:[10.1002/lpor.200810053](https://doi.org/10.1002/lpor.200810053)
- Xue, S.-J., Fang, L., Long, X.-M., Lu, Y., Wu, F., Li, W.-J., Zuo, J.-Q., Zhang, S.-F.: Influence of ITO, graphene thickness and electrodes buried depth on LED thermal–electrical characteristics using numerical simulation. *Chin. Phys. Lett.* **31**(2), 028501-1–028501-4 (2014). doi:[10.1088/0256-307x/31/2/028501](https://doi.org/10.1088/0256-307x/31/2/028501)
- Yeh, P., Yariv, A., Hong, C.-S.: Electromagnetic propagation in periodic stratified media. I. General theory. *JOSA* **67**(4), 423–438 (1976)
- Yu, Y., Wu, X.: Study of the generalized mixture rule for determining effective conductivity of two-phase stochastic models. *Appl. Geophys.* **7**(3), 210–216 (2010)